Expression of the FUS-CHOP Fusion Protein in Primary Mesenchymal Progenitor Cells Gives Rise to a Model of Myxoid Liposarcoma

Nicolò Riggi,[1] Luisa Cironi,[1] Paolo Provero,[3] Mario-Luca Suvà,[1] Jean-Christophe Stehle,[1] Karine Baumer,[1] Louis Guillou,[2] and Ivan Stamenkovic[1]

Divisions of [1]Experimental Pathology and [2]Anatomic Pathology Division, Institute of Pathology, University of Lausanne, Lausanne, Switzerland; and [3]Department of Genetics, Biology and Biochemistry, University of Turin, Turin, Italy

Abstract

A subset of sarcomas is associated with specific chromosomal translocations that give rise to fusion genes believed to participate in transformation and oncogenesis. Identification of the primary cell environment that provides permissiveness for the oncogenic potential of these fusion genes is essential to understand sarcoma pathogenesis. We have recently shown that expression of the EWS-FLI-1 fusion protein in primary mesenchymal progenitor cells (MPCs) suffices to develop Ewing's sarcoma-like tumors in mice. Because most sarcomas bearing unique chromosomal translocations are believed to originate from common progenitor cells, and because MPCs populate most organs, we expressed the sarcoma-associated fusion proteins FUS/TLS-CHOP, EWS-ATF1, and SYT-SSX1 in MPCs and tested the tumorigenic potential of these cells *in vivo*. Whereas expression of EWS-ATF1 and SYT-SSX1 failed to transform MPCs, FUS-CHOP–expressing cells formed tumors resembling human myxoid liposarcoma. Transcription profile analysis of these tumors revealed induction of transcripts known to be associated with myxoid liposarcoma and novel candidate genes, including *PDGFA*, whose expression was confirmed in human tumor samples. $MPC^{FUS\text{-}CHOP}$ and the previously described $MPC^{EWS\text{-}FLI\text{-}1}$ tumors displayed distinct transcription profiles, consistent with the different target gene repertoires of their respective fusion proteins. Unexpectedly, a set of genes implicated in cell survival and adhesion displayed similar behavior in the two tumors, suggesting events that may be common to primary MPC transformation. Taken together, our observations suggest that expression of FUS-CHOP may be the initiating event in myxoid liposarcoma pathogenesis, and that MPCs may constitute one cell type from which these tumors originate. (Cancer Res 2006; 66(14): 7016-23)

Introduction

Two major categories of mesenchyme-derived cancer include hematopoietic malignancies and sarcomas. Sarcomas comprise bone and soft tissue tumors, several of which arise in children and young adults. Although they account for <10% of all malignancies, sarcomas are among the most aggressive forms of cancer in that they have a high metastatic proclivity and are typically refractory to conventional chemotherapy and radiation therapy. Currently, relatively little is known about their origin, biological properties, and pathogenesis.

Sarcomas can be subdivided into two subclasses according to the genetic events that underlie or accompany their development. One subclass is associated with multiple complex chromosomal deletions, translocations, and duplications (1–3), whereas the other typically carries specific "signature" mutations. The majority of these are chromosomal translocations that lead to the generation of fusion proteins, most of which behave as aberrant transcription factors (1–3). Although expression of these fusion proteins is believed to underlie the pathogenesis of the bone and soft tissue tumors with which they are associated, the mechanism whereby they transform cells are still poorly understood. Equally incomplete is the understanding of the type of cellular environment that allows the fusion proteins to display their potential oncogenic properties. A major challenge to elucidating the pathogenesis of sarcomas, therefore, is the identification of the fusion protein/primary cell combination that underlies their development (2, 3).

Recently, we found that the EWS-FLI-1 fusion protein, which is associated with 85% of Ewing's sarcomas (also known as Ewing's family tumors or EFT) can transform primary wild-type bone marrow–derived mesenchymal progenitor cells (MPCs) to form Ewing's sarcoma–like tumors in mice (4). Moreover, EWS-FLI-1 expression in the absence of other pro-oncogenic events was sufficient to induce MPC transformation, suggesting that, in the appropriate cellular microenvironment, it may constitute the initiating event in EFT pathogenesis (4). Mesenchymal progenitor cells display a high degree of plasticity and can differentiate into osteocytes, adipocytes, neurons, and chondrocytes (5). Despite their bone marrow origin, MPCs can migrate to a broad range of tissues, including soft tissue compartments where most sarcomas develop (6). Based on these observations and the notion that sarcomas arise in pluripotent mesenchymal cells, we addressed the possibility that MPCs might provide the origin of other sarcomas associated with specific chromosomal translocations.

The *EWS* gene is the most frequent participant in chromosomal translocations that are specifically associated with sarcomas. Its fusion partners include FLI-1, ERG, ETV1, ETV4, and FEV (Ewing's sarcoma); ATF1 (clear cell sarcoma); WT1 (desmoplastic small round cell tumor); NR4A3 (myxoid chondrosarcoma); and CHOP/DDIT3 (myxoid liposarcoma; ref. 7). Interestingly, EWS shares functional properties with FUS/TLS (fused in sarcoma/translocated in sarcoma) that is also associated with sarcomas (8). Although less versatile than EWS, FUS can form fusion proteins with several partners, including *ATF1* (angiomatoid fibrous histiocytoma), *ERG* (Ewing's sarcoma and acute myeloid leukemia), *BBF2H7* (low-grade fibromyxoid

Note: Supplementary data for this article are available at Cancer Research Online (http://cancerres.aacrjournals.org/).

Requests for reprints: Ivan Stamenkovic, Division of Experimental Pathology, Institute of Pathology, University of Lausanne, CH-1011 Lausanne, Switzerland. Phone: 41-21-314-7136; Fax: 41-21-314-7110; E-mail: Ivan.Stamenkovic@chuv.hospvd.ch.

doi:10.1158/0008-5472.CAN-05-3979

sarcoma), and *CHOP*, t(12;16)(q13;p11) (myxoid liposarcoma; ref. 9). EWS and FUS/TLS contain structural features that are consistent with their implication in RNA processing (10–13). The NH_2-terminal domain of FUS/TLS binds to RNA polymerase II, whereas its COOH-terminal domain interacts with the transcription and translation factor Y-box binding protein -1. Within the FUS-CHOP fusion protein, the RNA-binding sequences of FUS are replaced by DNA-binding sequences and the basic leucine zipper domain of CHOP (11, 14). Similar to EWS, the NH_2-terminal portion of FUS that forms the fusion proteins contains potent transactivation domains (10, 15). Thus, as in EWS fusion proteins, transcription is mediated by FUS sequences, whereas the DNA-binding motifs are provided by the fusion partner (10, 15).

In light of the transforming potential displayed by EWS-FLI-1 and the structural and functional similarities between EWS and FUS, we addressed the effect of the myxoid liposarcoma–associated FUS-CHOP and clear cell sarcoma–associated EWS-ATF1 fusion proteins on MPC transformation and tumor development. Myxoid liposarcoma accounts for more than a third of liposarcomas, which amounts to about 10% of all adult soft tissue sarcomas (1). Recent studies suggest that myxoid liposarcoma express genes implicated in neural and osteocytic differentiation, supporting the notion that these tumors may be derived from mesenchymal progenitor cells (16, 17). The synovial sarcoma–associated fusion protein SYT-SSX1, which failed to display oncogenic properties in MPCs in previous experiments (4), was used as a negative control for FUS-CHOP and EWS-ATF1.

Expression of FUS/TLS-CHOP in MPCs resulted in their transformation with development of myxoid liposarcoma–like tumors. In contrast, MPCs expressing the EWS-ATF1 fusion protein failed to form tumors *in vivo*, as did SYT-SSX1 expressing cells. Our observations suggest that primary mesenchymal progenitor cells display selective permissiveness for sarcoma-associated fusion protein–mediated transformation, and that similar to EWS-FLI-1, FUS-CHOP expression can provide the single genetic event that is necessary and sufficient for the development of a defined soft tissue tumor from MPCs. Comparison of $MPC^{EWS\text{-}FLI\text{-}1}$ and $MPC^{FUS\text{-}CHOP}$ tumors revealed distinct transcription profiles, consistent with different target gene repertoires of the fusion proteins and a common gene expression signature that may be linked to primary mesenchymal cell transformation.

Materials and Methods

Cells. MPCs were isolated from bone marrow of adult C57BL/6 wild-type mice according to the methods described (4) and cultured on fibronectin-coated plates (Sigma, St. Louis, MO) in medium containing 2% dialyzed FCS (Sigma), 10 ng/mL epidermal growth factor (Sigma), 10 ng/mL PDGF-BB (R&D Systems, Minneapolis, MN), and leukemia inhibitory factor that was produced by the CHO LIF720D, LIF-producing cell line. MPCs were tested by fluorescence-activated cell sorting for mesenchymal stem cell marker expression before infection (following 4 weeks in culture or four passages) and after infection and selection (10 passages). In both cases, the MPCs were negative for the hematopoietic marker CD45 and CD11b; strongly positive for SCA-1, Thy1, CD13, and CD44; and weakly positive for CD117.

Cloning and reverse transcription-PCR. The cDNA clones encoding the human FUS-CHOP and EWS-ATF1 fusion genes were amplified from frozen human specimens of myxoid liposarcoma and clear cell sarcoma, respectively, by reverse transcription-PCR (RT-PCR). Amplification was done using Super Script one-step RT-PCR with the platinum Taq kit (Invitrogen, Carlsbad, CA) under the following cycling conditions: one cycle at 50°C for 30 minutes and 94°C for 2 minutes followed by 35 cycles of 94°C for 45 seconds, 55°C for 45 seconds, 72°C for 2 minutes, and a final extension of 72°C for 10 minutes. The sequences of primers used for amplification were as follows: hFUS forward *Bgl*II, AGATCTCCAC-CATGGCCTCAAACGATTATACC; hCHOP reverse *Xho*I (including a stop codon), CTCGAGTCATGCTTGGTGCAGATTCAC; hEWS forward *Bgl*II, GGAAGATCTCCACCATGGCGTCCACGGATTACAG; hATF1 reverse *Eco*RV (including a stop codon), ATATCTCAAACACTTTTATTGGAATAAAG.

The amplified fragments were digested with *Bgl*II and *Xho*I or *Bgl*II and *Eco*RV and inserted into the pMSCV Puro retroviral expression vector (BD Biosciences Clontech, Palo Alto, CA). The V5 epitope tag was added at the 3′ end of the FUS-CHOP sequence by PCR using the following primers: hFUS forward *Bgl*II, AGATCTCCACCATGGCCTCAAACGATTATACC; hCHOP V5 reverse (without a stop codon), AGGGTTAGGGATAGGCTTACCTTCGAAC-CGCGGGCCTGCTTGGTGCAGATT; V5 reverse *Hpa*I (including a stop codon), GTTAACTCACGTAGAATCGAGACCGAGGAGAGGGTTAGGGATAGGCTTACC.

The amplified fragment was digested with *Xho*I and *Hpa*I and inserted into the pMSCV Puro retroviral expression vector.

Plasmids were sequenced to verify cDNA integrity.

Retrovirus generation and infection. Expression of hFUS-CHOPV5 and hEWS-ATF1 in MPCs was achieved using a retroviral gene delivery method. Briefly, ecotropic packaging 293 cells were transfected either with fusion genes containing pMSCV Puro or an empty pMSCV Puro vector, using Superfect transfection reagent (Qiagen, Valencia, CA). Supernatants were collected after 72 hours, diluted 1:1 with MPCs medium containing 16 μg/mL of polybreen (Sigma), and added to six-well tissue culture plates containing 50% confluent MPCs. The plates were then centrifuged for 20 minutes at 1,800 rpm. RNA and proteins from infected cells were extracted at 24, 72 hours, and 10 days after infection. Expression of the fusion genes was tested at each time point by RT-PCR and Western blot (using the mouse anti-V5 or the rabbit anti-EWS antibody). The infected cells were selected as a bulk culture with 1.5 μg/mL puromycin for a minimum of 5 days and a maximum of 10 days.

cDNA array hybridization. Total RNA was extracted from each cell line using RNeasy Mini kit (Qiagen) according to the manufacturer's recommendations. The quality and the integrity of total RNA were verified by an Agilent RNA 600 nanoassay and by measuring the 260/280 absorbance ratio. Quality-tested total RNA was then amplified using the RiboAmp RNA Amplification kit (Arcturus, Mountain View, CA). After assessing the amplification by ethidium bromide agarose gel electrophoresis, the amplified RNA was processed using a reverse transcription–based method of label incorporation to yield labeled cDNA. For each sample, 5 μg of amplified RNA were used in the cDNA probe synthesis with Cy5-dCTP or Cy3-dCTP (Amersham Biosciences, Amersham, United Kingdom) and random primers. Probes were purified using a Mini Elute PCR purification kit (Qiagen) and concentrated using Centricon YM-30 filters (Amicon, Millipore, Billerica, MA). Expression analysis was done using the NIA 17k clone set (18), Quantifoil support array.[4] Hybridization was done in hybridization chambers (Corning Costar, Cambridge, MA) in a 64°C water bath for 16 hours.

cDNA array analysis. Following hybridization and washing, microarrays were imaged using a ScanArray 4000 scanner (Perkin-Elmer, Foster City, CA), and scanned slide images were converted to a tagged image file format. Fluorescence ratios for array elements were extracted by using ScanAlyze software,[5] and further primary data analysis was done using com.braju.sma routines in R statistical package.[6,7] Cy5 (red) and Cy3 (green) signal intensities were used to calculate M and A for every spot on each array. M is a measure of differential gene expression and is calculated as the log 2 of the red and green intensity ratio (i.e., log 2 Cy5/Cy3). A is a measure of the signal strength that was calculated as the mean of the log 2 red and green intensity: (log 2 Cy5 + log 2 Cy3) / 2. M values were normalized using the library sma in the statistical software package R[7] by the within-print-tip group Lowess normalization procedure (19). Quality control of slide hybridization was done using variables described on the corresponding web site.[8]

[4] For accurate description, see http://intranet.isrec.isb-sib.ch/microarrays/clones.html.
[5] http://rana.lbl.gov/EisenSoftware.htm.
[6] http://www.maths.lth.se/help/R/.
[7] http://www.r-project.org/.
[8] http://www.unil.ch/dafl.

Statistical analysis of the expression data. For each time point and cell line, five m17k microarrays (among which two were dye swaps) were done comparing *hFUS-CHOPV5* expressing with empty vector control cells. Expression data for each time point and cell line were analyzed with standard one-sample, two-sided *t* tests applied to the logarithm of the ratio of the expression levels of the *hFUS-CHOPV5* and the control sample. The null hypothesis is that the mean of such a logarithm is 0, and the alternate hypothesis is that the mean is not equal to 0.

The use of a standard statistical test (as opposed to methods based on cutoff on fold-change) allowed us to estimate the false discovery rate (FDR) of the lists of induced and repressed genes. This was done using the Benjamini-Hochberg method (20), in which the clones are sorted by increasing *t* test *P*, and the list thus obtained is truncated in correspondence of the last gene for which the FDR estimator is lower than a preset value. The FDR estimator is given by $(N \times C) / n$, where N is the total number of clones analyzed, C is the *t* test P of the gene, and n is its position in the list sorted by increasing P.

Western blot analysis. Cells were lysed for 20 minutes on ice in a nuclear lysis buffer containing 50 mmol/L Tris (pH 7.5), 0.5 mol/L NaCl, 1% NP40, 1% sodium deoxycholate, 0.1% SDS, 2 mmol/L EDTA, and complete protease inhibitors (Roche, Basel, Switzerland), and the lysates were then sonicated on ice thrice for 30 seconds. Samples were subjected to SDS-PAGE, and proteins were blotted onto polyvinylidene difluoride membranes (Millipore). Immunostaining was done after blocking with 5% nonfat dry milk, and bands were detected using a chemiluminescent substrate kit (Amersham Biosciences) according to the manufacturer's recommendations. Primary monoclonal mouse anti-V5 epitope (Invitrogen) or polyclonal rabbit anti-EWS (Bethyl Laboratories, Montgomery, TX) antibodies and secondary horseradish peroxidase–conjugated goat anti-mouse or anti-rabbit (Bio-Rad, Hercules, CA) antibodies were used.

Real-time quantitative RT-PCR. cDNA was obtained using an M-MLV reverse transcriptase and RNase H minus (Promega, Madison, WI). Typically, 500 ng of template total RNA and 250 ng of random hexamers were used per reaction. Real-time PCR amplification was done using a Taqman Universal PCR mastermix and Assays-On-Demand gene expression products in an ABI Prism 7700 instrument (Applied Biosystems, Foster City, CA). Relative quantitation of target, normalized with an endogenous control (cyclophyllin A), was done using a comparative C_t or a standard curve method (Applied Biosystems).

***In vitro* NVP-AEW541 sensitivity assays.** For the 3-(4,5-dimethylthiazol-2-yl)-2,5-diphenyltetrazolium bromide assay, MPCs cells were cultured in 24-well plates and treated with normal medium, 0.5 μmol/L NVP-AEW541, or solvent (DMSO) for 10 days. Cell sensitivity for the drug was tested with CellTiter AQueous Non-Radioactive Cell Proliferation Assay (Promega) according to the manufacturer's recommendations.

Tumorigenicity assays. Five-week-old BALB/cJHanHsd-SCID mice were obtained from Harlan (Indianapolis, IN). For each MPC cell population, 12 mice were injected s.c. with 1.5×10^6 cells stably expressing either hFUS-CHOPV5, hEWS-ATF1, hSYT-SSX1, or empty vector. Tumor growth was monitored weekly, and tumor-bearing mice were euthanized 6 weeks after injection. Six mice were injected s.c. with 1.5×10^6 cells from each independent MPCs $^{FUS\text{-}CHOP}$ tumor-derived cell population and sacrificed 2 weeks after injection. All tumors were resected at autopsy and sectioned for histologic analysis. All experimental protocols involving mice were approved by the Etat de Vaud, Service Vétérinaire, authorization no. VD1477.0.

Tumor explants. Tumor-bearing mice were euthanized, and the tumors were excised, disaggregated in 4 mL of PBS supplemented with 10 % fetal bovine serum + Ca^{2+} and Mg^{2+}, and resuspended for 40 minutes at 37°C in 15 mL of an enzymatic cocktail containing 2 mg collagenase VIII + 30 mg trypsin in 30 mL of PBS. The supernatants were then filtered and centrifuged for 6 minutes at $400 \times g$, and the resulting cellular pellets were plated in MPC medium without LIF, containing 1.5 μg/mL puromycin for tumor cell selection.

Immunohistochemistry. Paraffin-embedded sections of MPCs$^{FUS\text{-}CHOP}$- and MPCs$^{EWS\text{-}FLI\text{-}1}$-derived tumors were stained with mouse anti-human CD99 (1:40 dilution; Signet Laboratories, Dedham MA) and neural-specific enolase (NSE; 1:100 dilution; DAKO, Glostrup, Denmark) monoclonal antibody, or goat anti-human PDGF-A (1:100 dilution; R&D Systems). The latter antibody was also used to stain the human sarcoma paraffin sections. Horseradish peroxidase staining was done using biotin-conjugated horse anti-mouse or rabbit anti-goat immunoglobulin (DAKO) and revealed with a DAKO 3,3′-Diaminobenzidine kit (DAKO).

Results

MPCs expressing FUS-CHOP form tumors resembling myxoid liposarcoma. The FUS-CHOP, EWS-ATF1, and SYT-SSX cDNAs were isolated by RT-PCR from total RNA derived from frozen surgical specimens of human myxoid liposarcoma, clear cell sarcoma, and synovial sarcoma, respectively. The FUS-CHOP cDNA was amplified from a tumor containing the fusion of exon 5 of FUS to exon 2 of CHOP (type 2 fusion; ref. 1), which is seen in about 70% of cases, and sequences encoding the v5 tag were added to the 3′ end. Each cDNA was then inserted into the pMSCV retroviral vector, and the corresponding constructs were used to produce retroviruses and infect MPCs as described previously (4). Mesenchymal progenitor cells were derived from the bone marrow of wild-type C57BL/6 mice as described in Materials and Methods and characterized by a CD45-negative, CD11b-negative, CD44-positive, Thy1-positive, CD117 weakly positive, CD13 weakly positive, and Sca1 strongly positive phenotype (21, 22). Upon stimulation with appropriate growth factors, these cells differentiated into adipocytes, myocytes, chondrocytes, and neurons (21, 22) but failed to produce tumors in immunocompromised mice.

Bulk cultures of retrovirally infected MPC were selected for further experiments. Expression of each fusion protein was verified by Western blot analysis of lysates of the corresponding MPCs using anti-v5 or anti-EWS antibodies. All three fusion proteins were observed to be stably expressed (Fig. 1), and no major morphologic changes were noted in any of the retrovirally infected cells.

Ten days after infection each of the bulk MPC cultures was injected s.c. into a minimum of 12 severe combined immunodeficient mice. Three weeks following injection, all 12 mice that had received MPC$^{FUS\text{-}CHOP}$ cells developed visible tumors (Fig. 2*A*), and four animals were sacrificed for tumor analysis each week thereafter. By contrast, MPC$^{EWS\text{-}ATF1}$ and MPC$^{SYT\text{-}SSX1}$ failed to form tumors as late as 4 months after injection, when the experiment was terminated. The experiment was repeated with fresh batches of MPC, with and without the v5 tag and using different selection periods with identical results.

Human myxoid liposarcoma typically display variable cellularity, often containing lipogenic tumor cells surrounded by a myxoid stroma and numerous dilated capillaries (23). Histologic analysis revealed that the MPC$^{FUS\text{-}CHOP}$ tumors were composed of small, occasionally vacuolated cells embedded in a richly vascularized myxoid matrix (Fig. 2*B*; Supplementary Data S3), reminiscent of human myxoid liposarcoma (Fig. 2*B*; Supplementary Data S3). To determine whether the observed phenotype undergoes modifications with tumor progression, tumor-derived MPC$^{FUS\text{-}CHOP}$ cells were disaggregated and reinjected into mice. Although the second round tumors appeared more rapidly than their predecessors (Fig. 2*A*), their growth rate was only slightly higher than that of late stage first round tumors, whereas their histologic phenotype was comparable (data not shown). Importantly, expression of the FUS-CHOP protein was maintained in the first- and second-round tumor-derived cells (Fig. 1; data not shown). One possible explanation for the more rapid outgrowth of these second round tumors may be that because they were derived from cells that had adapted to the s.c. microenvironment, tumor take was facilitated. Although it is possible that these tumors incurred additional

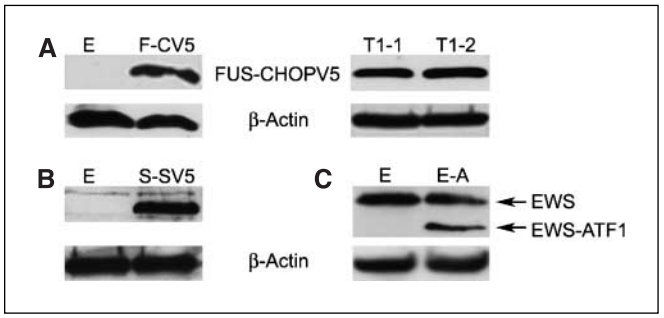

Figure 1. Western blot analysis of FUS-CHOP, SYT-SSX1, and EWS-ATF1 fusion protein expression. *A, left,* FUS-CHOPV5 expression in MPCs 10 days after infection with either empty (*lane E*) or FUS-CHOPV5 expressing vector (*lane F-CV5*). *Right,* expression of the FUS-CHOPV5 fusion protein in two independent $MPC^{FUS\text{-}CHOP\text{-}T1}$-derived cell populations (T1-1 and T1-2). *B* and *C,* expression of the SYT-SSX1V5 (*B*) and EWS-ATF1 (*C*) chimeric proteins in MPCs 10 days after infection with empty (*E*), SYT-SSXV5 (*S-SV5*), or EWS-ATF1 (*E-A*) expressing vectors.

genetic modifications that favor survival and growth, gene expression profile comparison between first- and second-round tumors failed to reveal changes that might reflect any obvious genetic events (data not shown).

Transcriptome modifications induced by FUS-CHOP in MPCs and $MPC^{FUS\text{-}CHOP}$ tumor cells. To determine the effect of FUS-CHOP on gene expression in MPCs, we compared transcription profiles of cells infected with FUS-CHOP containing retrovirus to those of corresponding cells infected with empty virus 24 and 72 hours as well as 14 days after infection. RNA was obtained from two independently FUS-CHOP–infected and two independently empty virus-infected cell populations, and expression of 17,000 cDNA clones was compared using the NIA-17K mouse cDNA array (18). Four microarrays were used to assess expression profile changes in each cell population. Expression data for each clone present on the microarray were analyzed with standard one-sample, two-sided *t* tests applied to the logarithm of the ratio of the expression levels of the $MPC^{FUS\text{-}CHOP}$ and MPC^{Vector} sample. This approach helped identify sets of *FUS-CHOP*–induced and repressed genes (Supplementary Data S1), and the false discovery rate (FDR) of each gene set was estimated by the Benjamini-Hochberg method as described in Materials and Methods. At 24 hours, 652 and 483 genes were respectively induced and repressed in response to FUS-CHOP expression with an FDR of 5%, whereas 610 and 555 genes, respectively, displayed induction and repression at 72 hours but with a 10% FDR (Supplementary Data S1). At 14 days, only 15 and 25 genes displayed induction and repression, respectively, with a 20% FDR. Interestingly, whereas infection of MPCs with retrovirus containing EWS-FLI-1 resulted in robust insulin-like growth factor-1 (IGF-1) induction (4), up-regulation of *PDGFA* but not of IGF-1 was observed in FUS-CHOP–expressing cells (Fig. 3).

To obtain clues as to the mechanisms that underlie FUS-CHOP–induced tumorigenicity, we compared the gene expression profile of cells derived from the first-round $MPC^{FUS\text{-}CHOP}$ tumors to their preinjection counterparts. RNA was obtained from two independently FUS-CHOP–infected and two independent tumor-derived cell populations, and expression of 17,000 cDNA clones was compared using the NIA-17K mouse cDNA array as above. Five microarrays were used to assess expression profile changes in each cell population. The gene expression pattern of $MPC^{FUS\text{-}CHOP}$ tumors compared with that of $MPC^{FUS\text{-}CHOP}$ cells before injection included repression of *CTGF, PERP*, and *TFPI* and induction of transcripts encoding growth factors (*PDGFA* and *HGF*), cytokines (*IL6*), growth factor receptors (*MET*), cell cycle regulators (*CDK4* and *MDM2*), proteolytic enzymes *(MMP-11, CTSD*, and *PLAT*), and factors implicated in adipocyte differentiation, including *ADFP, FASN, HMGCR*, and *RGS2* (Fig. 3*A-C*; refs. 24, 25), possibly explaining, in part, the histologic phenotype of the tumors. Among these genes, *CD24, LXN, CD1D1, PLTP, DAF1, HOXD3*, and *ADM* were found to be induced in NIH-3T3 cells by FUS-CHOP (Fig. 3*B*; ref. 17). Association of the cell cycle regulators *CDK4, MDM2* (26), the oncogene *MET* (27), fatty acid synthase (*FASN*; ref. 24), and *IL6* (28) with myxoid liposarcoma (Fig. 3*C*) was established by immunohistochemical studies on myxoid liposarcoma samples.

Induction of *PDGFA* had not been reported in myxoid liposarcomas previously, which prompted us to validate its expression by quantitative real-time PCR analysis and assess PDGFα expression in $MPC^{FUS\text{-}CHOP}$ tumors and human myxoid liposarcomas by immunohistochemistry. Consistent with the quantitative real-time PCR data (Fig. 3*C*), $MPC^{FUS\text{-}CHOP}$ tumors stained positively with anti-PDGFα antibody as did all 10 samples of human myxoid liposarcoma tested (Fig. 3*D*). By contrast, synovial sarcoma, Ewing's sarcoma, and chondrosarcoma did not display PDGFα expression as detected by immunohistochemistry, whereas alveolar rhabdomyosarcoma showed only marginal reactivity with the antibody (Fig. 4).

MPCs provide a unique model system to study myxoid liposarcoma and EFT development. Having recently observed that MPCs expressing the EWS-FLI-1 fusion protein form Ewing sarcoma–like tumors in mice (4), we compared the effect of FUS-CHOP and EWS-FLI-1 on MPCs. We first assessed the expression profile changes of cells infected with each fusion gene at 24 hours, when the number of transcripts displaying expression change was the highest (4). As might be expected, major differences in the

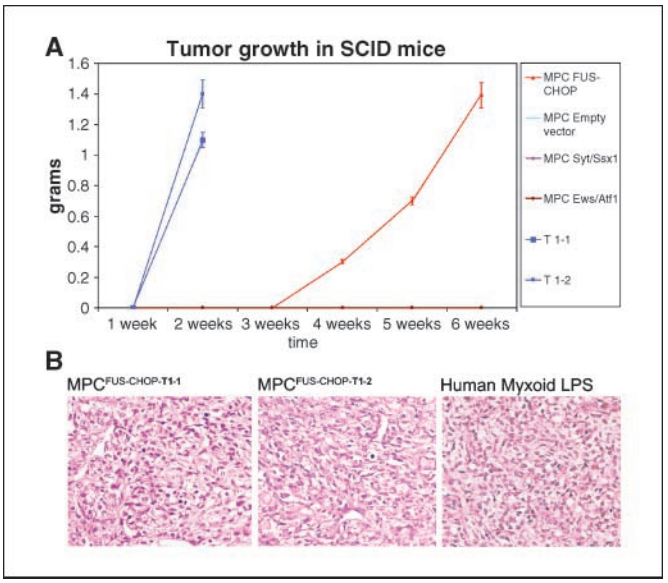

Figure 2. Growth and histology of $MPC^{FUS\text{-}CHOP}$ tumors. *A,* tumor growth in severe combined immunodeficient (*SCID*) mice injected with MPCs expressing FUS-CHOPV5, SYT-SSX1, EWS-ATF1, or empty vector. Four mice were sacrificed at 4, 5, and 6 weeks, and tumors were resected and weighed. Two of the tumors removed 6 weeks after injection were dissociated, and the cells were assessed for FUS-CHOPV5 expression, as shown in Fig. 1*A*. These cells ($MPC^{FUS\text{-}CHOP\text{-}T1.1}$ and $MPC^{FUS\text{-}CHOP\text{-}T1.2}$) were reinjected, and the resulting tumors were removed 2 weeks later. *Points,* mean tumor weight; *bars,* SD. *B,* histology of the $MPC^{FUS\text{-}CHOP}$ tumors is reminiscent of that of human MLPS, characterized by the presence of round cells surrounded by an abundant, and richly vascularized myxoid stroma. H&E staining. Magnification, ×100.

A

Clone ID	Gene symbol	Clone name	m value	t-test p value
		Induced genes		
H3144F06	Adfp	adipose differentiation related protein	2.42115	0.001348015
P566	Pdgfa	platelet derived growth factor, alpha	1.69742	6.99412E-05
H3146C02	Pdgfa	platelet derived growth factor, alpha	1.46917	5.00088E-05
P218	Hgf	hepatocyte growth factor	1.50525	0.000973888
H3110A02	Gfra1	glial cell line derived neurotrophic receptorα1	1.9441	0.007165476
T240	Rgs2	regulator of G-protein signaling 2	4.092375	0.000164043
H3032C10	Hmgcr	3-hydroxy-3-methylglutaryl-Coenzyme A	0.720625	0.000282944
P377	Mmp11	matrix metalloproteinase 11	2.101125	0.00432973
H3008H06	Ctsd	cathepsin D	1.993275	0.000163981
P625	Ctsd	cathepsin D	1.943575	0.005794607
H3080H11	Plat	plasminogen activator, tissue	1.869025	0.002568401
P408	Plat	plasminogen activator, tissue	1.61125	0.001521668
		Repressed genes		
P654	Ctgf	connective tissue growth factor	-4.907775	6.82987E-06
H3029F01	Perp	PERP, TP53 apoptosis effector	-2.337525	0.000544062
H3129H09	Tfpi	tissue factor pathway inhibitor	-1.829225	0.005508974
H3159G03	Tfpi	tissue factor pathway inhibitor	-1.400225	0.000676885

B

Clone ID	Gene symbol	Clone name	m value	t-test p value
H3155C06	Cd24a	CD24a antigen	2.926275	0.004170171
H3132E07	Lxn	latexin	1.72245	0.000881888
H3079C04	Cd1d1	CD1d1 antigen	1.367425	0.017043435
T190	Pitp	phospholipid transfer protein	1.17505	0.017546029
P627	Daf1	decay accelerating factor 1	0.868075	0.025117029
P688	Hoxd3	homeo box D3	0.738425	0.003886992
H3013H04	Adm	adrenomedullin	0.7005	0.008936805

C

Clone ID	Gene symbol	Clone name	m value	t-test p value
P372	Met	met proto-oncogene	0.60495	0.026053436
T076	Fasn	fatty acid synthase	0.757125	0.000664322
H3051D04	Mdm2	transformed mouse 3T3 cell double minute 2	0.8085	0.005532716
H3107F02	Cdk4	cyclin-dependent kinase 4	0.73645	0.01737568
T280	Il6	interleukin 6	1.523425	0.012555151

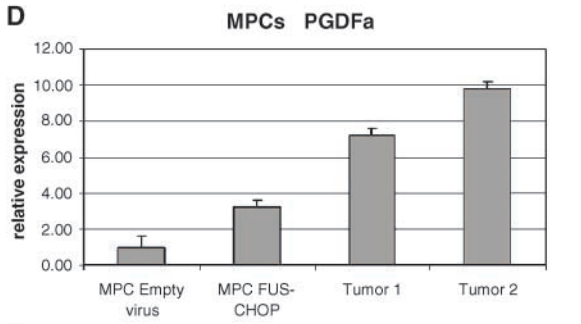

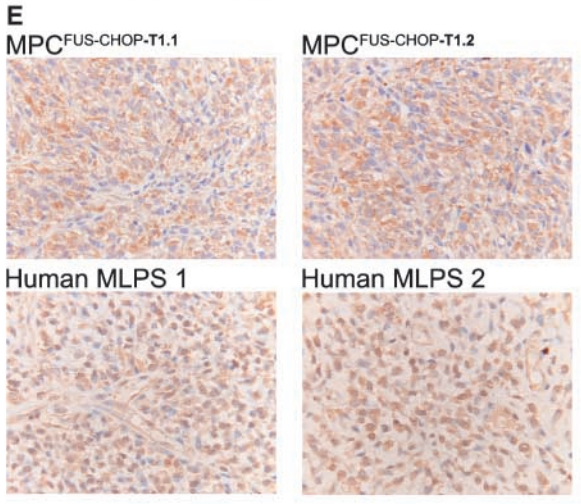

Figure 3. Transcription profile comparison between MPC$^{FUS-CHOP}$ and the corresponding tumor-derived cells and immunohistochemical assessment of PDGFα expression in MPC$^{FUS-CHOP-T1}$ and human MLPS. *A,* summary of genes potentially relevant to tumor pathogenesis that were induced and repressed in MPC$^{FUS-CHOPT1}$ tumor-derived cells in comparison to MPC$^{FUS-CHOP}$ cells before injection into mice. *B,* summary of genes induced in MPC$^{FUS-CHOP-T1}$ reported to be induced by FUS-CHOP expression in NIH-3T3 cells. *M* values indicate log 2 fold induction/repression. *C,* summary of genes induced in MPC$^{FUS-CHOP-T1}$ reported to be associated with MLPS in immunohistochemical studies and suggested to be implicated in the pathogenesis of human MLPS. *D,* histogram representation of mouse PDGFA transcript induction in MPC$^{FUS-CHOP}$ and MPC$^{FUS-CHOP-T1}$ compared with their empty vector–infected counterparts, as assessed by real-time PCR normalized to cyclophyllin A. *Columns,* mean of three separate determinations done in triplicate; *bars,* SD. *E,* PDGFα expression in two independent MPC$^{FUS-CHOP-T1}$ tumors and two unrelated human MLPS. Magnification, ×200.

composition of the induced and repressed transcripts in response to the two fusion proteins were observed (Supplementary Data S1). To further highlight this difference, we compared the number of genes that displayed similar or opposite expression changes in response to the two fusion proteins. We found that at 24 hours, only 17 transcripts displayed similar movement in response to both fusion proteins: 10 being induced and 7 repressed (Supplementary Data S1). By contrast, 124 genes that were induced in EWS-FLI-1–infected cells were repressed in FUS-CHOP–infected counterparts, whereas 212 transcripts displayed the inverse behavior (Supplementary Data S1).

Consistent with the observed difference in the early response of MPCs to FUS-CHOP and EWS-FLI-1, the morphology and transcription profile of MPC$^{EWS-FLI-1}$ and MPC$^{FUS-CHOP}$ tumors were divergent. Histologically, the tumors were distinct, with the former being characterized by sheets of small round blue cells and the latter by small often vacuolated cells with a richly vascularized myxoid matrix (Fig. 5). NSE expression, which is associated with EFTs and MPC$^{EWS-FLI-1}$ tumors, was not observed in MPC$^{FUS-CHOP}$ tumors (Fig. 5). Conversely, MPC$^{FUS-CHOP}$ tumor-associated PDGFα expression was lacking in MPC$^{EWS-FLI-1}$ counterparts (Fig. 5).

Comparison of MPC$^{FUS-CHOP}$ and MPC$^{EWS-FLI-1}$ tumor transcriptomes showed marked differences with respect to genes that bear potential relevance to the pathogenesis of each tumor type (Supplementary Data S2). Importantly, several genes, including the adipocytic differentiation markers FASN, HMGCR, and RGS2, that were induced in MPC$^{FUS-CHOP}$ tumors were repressed in MPC$^{EWS-FLI-1}$ tumor cells (Fig. 6*A*). The tumors also displayed different growth factor repertoires: IGF-1 being strongly induced in MPC$^{EWS-FLI-1}$ but not in MPC$^{FUS-CHOP}$ cells and tumors, and PDGFα being induced in MPC$^{FUS-CHOP}$ tumors but repressed in MPC$^{EWS-FLI-1}$ counterparts (Fig. 6*B*; Supplementary Data S2). Consistent with these observations, MPC$^{FUS-CHOP}$ tumors did not recapitulate the high sensitivity displayed by MPC$^{EWS-FLI-1}$ tumors to IGF-1R blockade by the pyrrolo[2,3-*d*] pyrimidine derivative small molecular weight kinase inhibitor AEW541 (refs. 4, 29; Fig. 6*C*).

Interestingly, several genes found to be induced or repressed in tumors derived from transformed MPCs were shared by MPC$^{EWS-FLI-1}$ and MPC$^{FUS-CHOP}$ tumor cells. They included *YAP, BIRC2*, and *TGFBI*, which were induced, and *LUM, ALCAM, JAM2, JAM3, CAH11, FATH*, and *CALDESMON1*, which were repressed in both tumor types (Fig. 6*D*). Induction and repression of selected transcripts within this group, including ALCAM, JAM2, LUM, BIRC2, and YAP, were validated in MPC$^{FUS-CHOP}$ tumor cells by quantitative RT-PCR analysis (Fig. 6*E*).

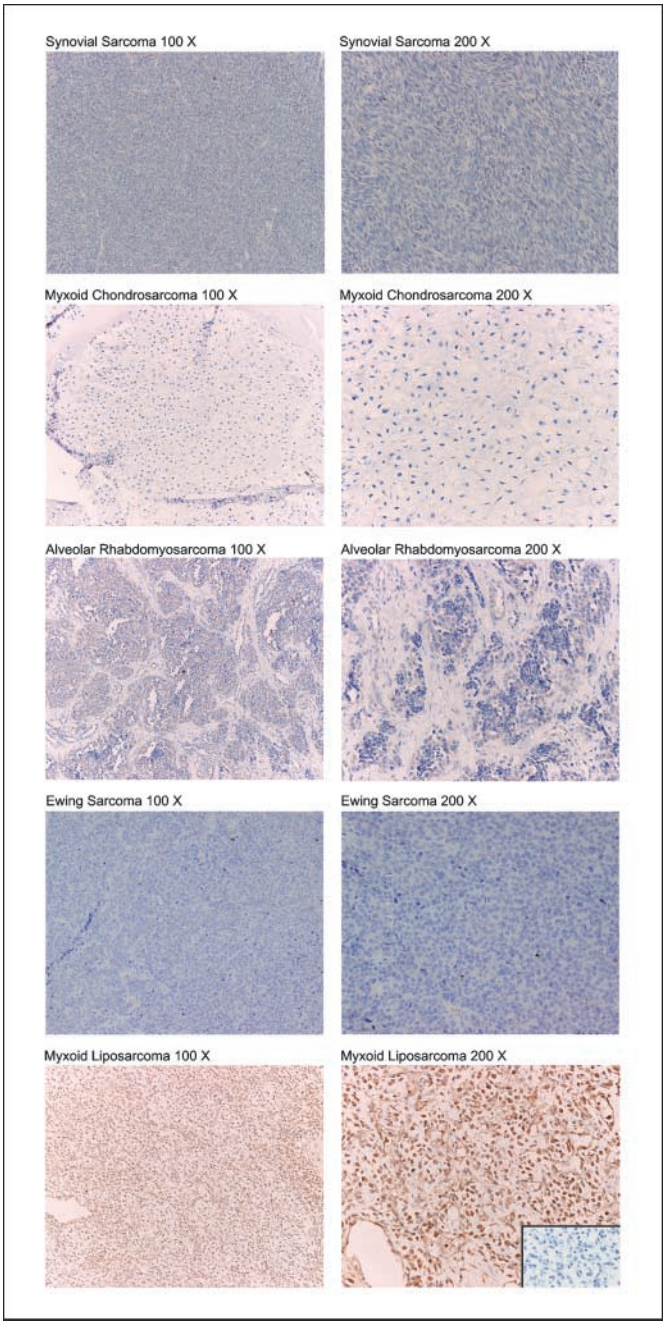

Figure 4. Immunohistochemical assessment of PDGFα expression, using anti-PDGFα antibody, in a selection of human sarcomas bearing specific chromosomal translocations. Magnifications are indicated. *Inset,* staining with an unrelated, isotype-matched control antibody.

Discussion

FUS-CHOP has been observed to induce transformation in cell type–specific fashion (9), suggesting that permissiveness for its oncogenicity is a function of the cellular context. Our present work provides evidence that primary MPCs provide a permissive environment for FUS-CHOP–mediated transformation, and that MPCs expressing FUS-CHOP form tumors resembling human myxoid liposarcoma. Coupled to our recent finding that EWS-FLI-1 expression in MPCs leads to the formation of EFT-like tumors, these observations raise the possibility that myxoid liposarcoma and EFTs may originate from the same or closely related cells, albeit at different locations within the body. The preferential bone and soft tissue localization of EFTs and myxoid liposarcoma, respectively, may depend, in part, on local microenvironment-dependent modulation of MPC susceptibility to transformation by the corresponding fusion proteins and in part on the ability of the transformed cells to adapt to constraints imposed by the physiologic properties of the surrounding tissue.

Similar to the effect of EWS-FLI-1, expression of FUS-CHOP alone was sufficient to transform MPCs and induce them to form tumors *in vivo*. Although it is widely held that development of solid tumors requires an average of three genetic events (30), many of the experiments on which this view is based were done in differentiated cells with limited plasticity and potential for self-renewal. Mesenchymal progenitor and hematopoietic stem cells retain high self-renewal proclivity, survival capacity, and migratory and invasive properties (31, 32), all of which constitute features of malignant cells. Our present observations are consistent with the possibility that in such an environment a single, appropriately targeted, genetic event may suffice to induce transformation. Attempts to develop transgenic models of liposarcoma using FUS-CHOP constructs driven by adipocyte-specific promoters failed, further suggesting that FUS-CHOP may require a mesenchymal progenitor/stem cell environment to exert its oncogenic potential. Consistent with this notion, transgenic mice engineered to express FUS-CHOP under the control of the ubiquitous E1Fα promoter, which we found to be functional in MPCs (data not shown), developed liposarcomas that resemble their human counterpart (33). Up-regulation of neuronal transcripts *PN-1, Neuronatin*, and *RET* in myxoid liposarcoma cells compared with normal adipocytes (16, 34) add further support to a mesenchymal protenitor/stem cell origin of myxoid liposarcoma.

Transcriptome analysis of $MPC^{FUS\text{-}CHOP}$ tumor cells revealed up-regulation of genes observed to be associated with myxoid liposarcoma and FUS-CHOP–transfected NIH-3T3 cells. Several of these genes, including *MDM2* (26), *CDK4* (35), and *HGFR* (c-met; ref. 27), are believed to participate in myxoid liposarcoma development. The same may hold true for PDGFα, which has a potent promigratory and growth-promoting effect on mesenchymal cells, and whose association with myxoid liposarcoma was a novel discovery in this study. Although PDGFα expression is associated with a variety of malignancies (36), its robust induction in MPCs by FUS-CHOP expression and presence in myxoid liposarcoma suggests a possible role in the pathogenesis of these tumors, much as IGF-1 seems to be implicated in the pathogenesis of Ewing's sarcoma growth, without being EFT specific.

Our present observations cannot predict which of the induced/suppressed genes are direct FUS-CHOP targets and which are indirectly affected by FUS-CHOP, possibly secondary to FUS-CHOP–induced differentiation or transformation. However, it is likely that a combination of both direct and indirect targets contributes to $MPC^{FUS\text{-}CHOP}$ tumor development. Moreover, induction of genes that are associated with myxoid liposarcoma and proposed to participate in its pathogenesis supports the notion that $MPC^{FUS\text{-}CHOP}$ tumors constitute a relevant model of myxoid liposarcoma.

Direct comparison of the effect of FUS-CHOP and EWS-FLI-1 expression in MPCs revealed major differences not only in the altered transcript repertoire but in the inverse response of >300 genes to the two fusion proteins. Comparisons of $MPC^{FUS\text{-}CHOP}$ to $MPC^{EWS\text{-}FLI\text{-}1}$ tumors further highlighted the difference in

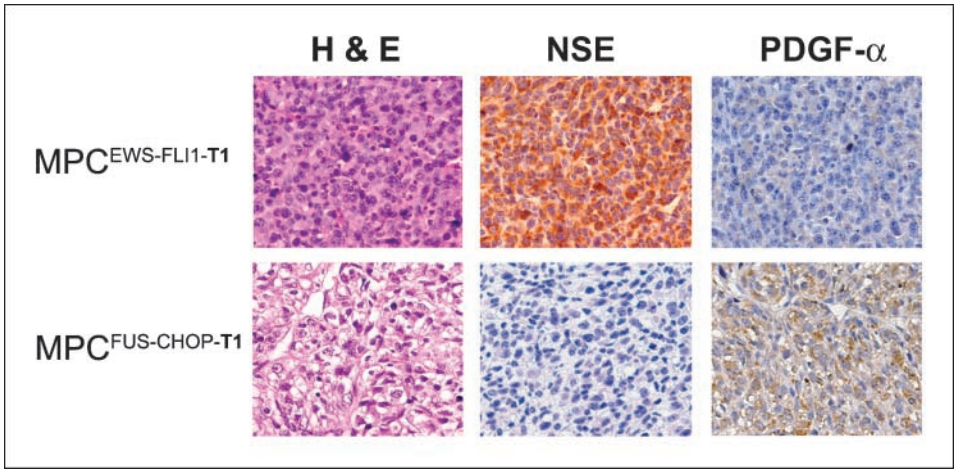

Figure 5. Histologic comparison of $MPC^{EWS\text{-}FLI\text{-}1\text{-}T1}$ and $MPC^{FUS\text{-}CHOP\text{-}T1}$ tumors, showing different morphology as assessed by H&E staining and differential expression of NSE and PDGFα as assessed using by immunohistochemistry using corresponding antibodies. Magnification, ×200.

EWS-FLI-1– and FUS-CHOP–mediated events. In addition to different histologic phenotypes, the tumors displayed distinct gene expression profiles consistent with the notion that despite a shared cell of origin, different signaling pathways underlie the pathogenesis of each tumor type. Thus, $MPC^{FUS\text{-}CHOP}$ tumors expressed *PDGFα, HGF*, and *GFRA1* but did not up-regulate *IGF-1* and, in contrast to $MPC^{EWS\text{-}FLI\text{-}1}$ tumors, displayed only moderate sensitivity to IGF-1R blockade (4). Moreover, adipose tissue differentiation genes associated with $MPC^{FUS\text{-}CHOP}$ tumors, including *FASN, HMGCR*, and *RGS2*, were repressed in $MPC^{EWS\text{-}FLI\text{-}1}$ tumor cells consistent with the notion that EWS-FLI-1 blocks adipocyte differentiation in MPCs (37). The absence of peroxisome proliferator-activated receptor γ (PPARγ) induction suggests a partial adipose lineage differentiation block in $MPC^{FUS\text{-}CHOP}$ tumors as well, consistent with the proposed effect of FUS-CHOP on PPARγ activity (32, 38–40).

Interestingly, many of the reported EWS-FLI-1 target genes and myxoid liposarcoma–associated genes were expressed in first round tumor cells but not in MPCs bearing the fusion proteins before injection. A possible explanation may be that a combination of transformation and *in vivo* growth conditions enables EWS-FLI-1 and FUS-CHOP bearing MPCs to express direct and indirect target genes of their respective fusion proteins. This notion is supported by the observation that EWS-FLI-1 expression resulted in the induction of several target genes in NIH-3T3 cells (41) but not in primary fibroblasts (42, 43).

Whereas distinct transcription profiles of $MPC^{EWS\text{-}FLI\text{-}1}$ and $MPC^{FUS\text{-}CHOP}$ tumors could be anticipated, based on different

A

Genes involved in adipocyte differentiation induced in MPC FUS-CHOP-T1, repressed in MPC EWS-FLI1-T1

			MPC EWS-FLI1-T1		MPC FUS-CHOP-T1	
Clone ID	Gene symbol	Clone name	m value	t-test p value	m value	t-test p value
T240	Rgs2	regulator of G-protein signaling 2	-0.82305	0.09214259	4.092375	0.000164043
H3094E10	Sc4mol	sterol-C4-methyl oxidase-like	-1.632	0.002816072	1.344775	0.000457112
T076	Fasn	fatty acid synthase	-1.00452	0.00362682	0.757125	0.000684322
H3032C10	Hmgcr	3-hydroxy-3-methylglutaryl-CoenzymeA red	-1.0361	7.88855E-05	0.720625	0.000282944

B

Clone ID	Gene symbol	Clone name	m value	t-test p value
		MPC EWS-FLI1-T1		
H3099C09	Igf1	insulin-like growth factor 1	1.54812	0.005997954
N750	Igf1	insulin-like growth factor 1	1.2216	0.008791687
		MPC FUS-CHOP-T1		
P566	Pdgfa	platelet derived growth factor, alpha	-0.85382	0.002974542
H3146C02	Pdgfa	platelet derived growth factor, alpha	-0.83255	0.000553246

C

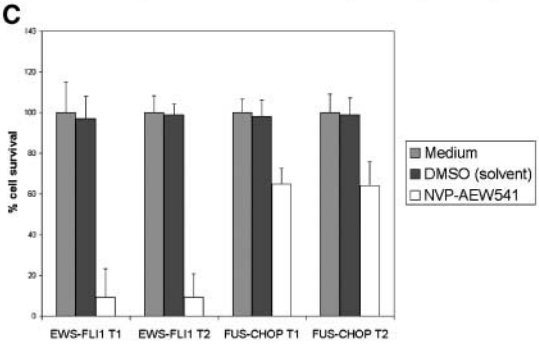

D

			MPC EWS-FLI1		MPC FUS-CHOP	
Clone ID	Gene symbol	Clone name	m value	t-test p value	m value	t-test p value
		Induced genes				
H3089H07	Yap	yes-associated protein	4.27295	0.000610493	4.34185	3.71062E-05
H3100E04	Birc2	baculoviral IAP repeat-containing 2	4.04415	0.002208851	4.09007	0.002031658
H3074A02	Birc2	baculoviral IAP repeat-containing 2	4.01705	0.002562297	4.28742	0.000434363
H3114E06	Tgfbi	transforming growth factor, beta induced	2.54197	0.001324279	5.66925	0.000191707
		Repressed genes				
P114	Lum	lumican	-3.5621	0.000694294	-3.4834	0.000200025
H3061D06	Fath	fat tumor suppressor homolog	-1.84342	0.003804202	-2.11422	0.000875051
H3120H03	Alcam	activated leukocyte cell adhesion molecule	-1.88667	0.026041564	-1.23617	0.005511504
H3109B09	Jam2	junction adhesion molecule 2	-1.92287	0.008189394	-3.4192	1.47183E-05
H3087H01	Jam2	junction adhesion molecule 2	-1.51805	0.008191939	-3.32077	0.000333239
H3107H01	Jam3	junction adhesion molecule 3	-1.12252	0.097776752	-2.08687	0.001440689
H3149F09	Cdh11	cadherin 11	-1.10992	0.00373099	-2.70787	3.84569E-05
H3022A11	Cald1	caldesmon 1	-1.09392	0.002242093	-2.39442	0.002124723

E

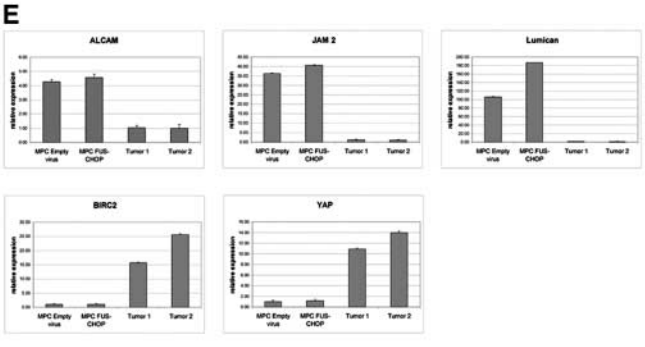

Figure 6. Transcription profile comparison between $MPC^{EWS\text{-}FLI\text{-}1\text{-}T1}$ and $MPC^{FUS\text{-}CHOP\text{-}T1}$. *A,* summary of transcripts involved in adipocyte differentiation that re induced in $MPC^{FUS\text{-}CHOP\text{-}T1}$ but repressed in $MPC^{EWS\text{-}FLI\text{-}1\text{-}T1}$ tumors compared with the corresponding cells before injection. *B,* direct transcript profile comparison between $MPC^{EWS\text{-}FLI\text{-}1\text{-}T1}$ and $MPC^{FUS\text{-}CHOP\text{-}T1}$ tumor cell RNA shows EWS-FLI-1–associated IGF-1 and FUS-CHOP–associated PDGFA induction. *C,* $MPC^{EWS\text{-}FLI\text{-}1\text{-}T1}$- and $MPC^{FUS\text{-}CHOP\text{-}T1}$-derived cell survival after exposure to 0.5 μg/mL NVP-AEW541 for 72 hours. *Columns,* mean of three separate determinations done in triplicate; *bars* SD. *D,* summary of genes relevant to transformation and tumor development that were differentially expressed between tumor-derived and preinjection MPC, shared by $MPC^{EWS\text{-}FLI\text{-}1\text{-}T1}$ and $MPC^{FUS\text{-}CHOP\text{-}T1}$ tumors. *E,* histogram representation of induced and repressed transcripts in $MPC^{FUS\text{-}CHOP\text{-}T1}$, selected from the list shown in (*D*), as assessed by real-time PCR normalized to cyclophyllin A. All experiments were done in triplicate. *Columns,* mean of triplicates of three separate determinations; *bars,* SD.

target gene specificity of the respective fusion proteins, the shared expression profile of several genes that may be relevant to oncogenesis were unexpected. Both tumor types were associated with induction of yes-associated protein (YAP) and BIRC2, which are believed to be involved in promoting cell survival. Both tumors also displayed repression of genes encoding lumican, fat-associated tumor suppressor, caldesmon, and the adhesion receptors ALCAM, Jam-2 and Jam-3, and cadherin 11. Repression of lumican, a small secreted protoglycan, has been observed to augment tumor cell proliferation (44, 45), whereas loss of adhesion receptors may facilitate cell migration and invasion. The observed induction and suppression of genes common to the two tumors may constitute a transcription profile that reflects important events in mesenchymal cell transformation. It is noteworthy that this putative expression signature was unaffected by the duration of tumor growth, being detected in $MPC^{FUS\text{-}CHOPT1}$ and $MPC^{EWS\text{-}FLI\text{-}1T1}$, respectively, 6 and 15 weeks following injection of the corresponding cells.

Taken together, our observations support the notion that expression of FUS-CHOP in the appropriate cellular environment may be the initiating event in myxoid liposarcoma development. Coupled to our recent report that EWS-FLI-1 expression transforms primary MPCs, the present study indicates that transformation of MPCs may be induced by single, selected genetic events, and that MPCs may provide a common origin of both EFTs and myxoid liposarcomas. MPC-derived tumor models may facilitate elucidation of the mechanisms, whereby FUS-CHOP and EWS-FLI-1 transform primary mesenchymal cells and provide new insight into the molecular pathogenesis of some of the most aggressive malignancies.

Acknowledgments

Received 11/7/2005; revised 3/30/2006; accepted 4/28/2006.

Grant support: Swiss National Science Foundation, Oncosuisse grant OCS 01656, and the Molecular Oncology National Centre for Competence in Research.

The costs of publication of this article were defrayed in part by the payment of page charges. This article must therefore be hereby marked *advertisement* in accordance with 18 U.S.C. Section 1734 solely to indicate this fact.

References

1. Sandberg AA. Updates on the cytogenetics and molecular genetics of bone and soft tissue tumors: liposarcoma. Cancer Genet Cytogenet 2004;155:1–24.
2. Mackall CL, Meltzer PS, Helman LJ. Focus on sarcomas. Cancer Cell 2002;2:175–8.
3. Helman LJ, Meltzer P. Mechanisms of sarcoma development. Nat Rev Cancer 2003;3:685–94.
4. Riggi N, Cironi L, Provero P, et al. Development of Ewing's sarcoma from primary bone marrow-derived mesenchymal progenitor cells. Cancer Res 2005;65:11459–68.
5. Jiang Y, Jahagirdar BN, Reinhardt RL, et al. Pluripotency of mesenchymal stem cells derived from adult marrow. Nature 2002;418:41–9.
6. Barry FP, Murphy JM. Mesenchymal stem cells: clinical applications and biological characterization. Int J Biochem Cell Biol 2004;36:568–84.
7. Bennicelli JL, Barr FG. Chromosomal translocations and sarcomas. Curr Opin Oncol 2002;14:412–9.
8. Morohoshi F, Ootsuka Y, Arai K, et al. Genomic structure of the human RBP56/hTAFII68 and FUS/TLS genes. Gene 1998;221:191–8.
9. Perez-Mancera PA, Sanchez-Garcia I. Understanding mesenchymal cancer: the liposarcoma-associated FUS-DDIT3 fusion gene as a model. Semin Cancer Biol 2005;15:206–14.
10. Rabbitts TH, Forster A, Larson R, Nathan P. Fusion of the dominant negative transcription regulator CHOP with a novel gene FUS by translocation t(12;16) in malignant liposarcoma. Nat Genet 1993;4:175–80.
11. Crozat A, Aman P, Mandahl N, Ron D. Fusion of CHOP to a novel RNA-binding protein in human myxoid liposarcoma. Nature 1993;363:640–4.
12. Goransson M, Wedin M, Aman P. Temperature-dependent localization of TLS-CHOP to splicing factor compartments. Exp Cell Res 2002;278:125–32.
13. Zinszner H, Albalat R, Ron D. A novel effector domain from the RNA-binding protein TLS or EWS is required for oncogenic transformation by CHOP. Genes Dev 1994;8:2513–26.
14. Ron D, Habener JF. CHOP, a novel developmentally regulated nuclear protein that dimerizes with transcription factors C/EBP and LAP and functions as a dominant-negative inhibitor of gene transcription. Genes Dev 1992;6:439–53.
15. Sanchez-Garcia I, Rabbitts TH. Transcriptional activation by TAL1 and FUS-CHOP proteins expressed in acute malignancies as a result of chromosomal abnormalities. Proc Natl Acad Sci U S A 1994;91:7869–73.
16. Thelin-Jarnum S, Lassen C, Panagopoulos I, Mandahl N, Aman P. Identification of genes differentially expressed in TLS-CHOP carrying myxoid liposarcomas. Int J Cancer 1999;83:30–3.
17. Schwarzbach MH, Koesters R, Germann A, et al. Comparable transforming capacities and differential gene expression patterns of variant FUS/CHOP fusion transcripts derived from soft tissue liposarcomas. Oncogene 2004;23:6798–805.
18. Tanaka TS, Jaradat SA, Lim MK, et al. Genome-wide expression profiling of mid-gestation placenta and embryo using a 15,000 mouse developmental cDNA microarray. Proc Natl Acad Sci U S A 2000;97:9127–32.
19. Yang YH, Dudoit S, Luu P, et al. Normalization for cDNA microarray data: a robust composite method addressing single and multiple slide systematic variation. Nucleic Acids Res 2002;30:e15.
20. Benjamini Y, Hochberg Y. Controlling the false discovery rate: a practical and powerful approach to multiple testing. Journal of the Royal Statistical Society, Series B Methodological 1995;57:289–300.
21. Peister A, Mellad JA, Larson BL, Hall BM, Gibson LF, Prockop DJ. Adult stem cells from bone marrow (MSCs) isolated from different strains of inbred mice vary in surface epitopes, rates of proliferation, and differentiation potential. Blood 2004;103:1662–8.
22. Sun S, Guo Z, Xiao X, et al. Isolation of mouse marrow mesenchymal progenitors by a novel and reliable method. Stem Cells 2003;21:527–35.
23. Kempson RL, Fletcher CD, Evans HL, Hendrickson MR, Sibley RK. Tumors of the soft tissues. Vol. 30. Bethesda: Armed Forces Institute of Pathology; 1998.
24. Takahiro T, Shinichi K, Toshimitsu S. Expression of fatty acid synthase as a prognostic indicator in soft tissue sarcomas. Clin Cancer Res 2003;9:2204–12.
25. Nishizuka M, Honda K, Tsuchiya T, Nishihara T, Imagawa M. RGS2 promotes adipocyte differentiation in the presence of ligand for peroxisome proliferator-activated receptor gamma. J Biol Chem 2001;276:29625–7.
26. Dei Tos AP, Piccinin S, Doglioni C, et al. Molecular aberrations of the G_1-S checkpoint in myxoid and round cell liposarcoma. Am J Pathol 1997;151:1531–9.
27. Wallenius V, Hisaoka M, Helou K, et al. Over-expression of the hepatocyte growth factor (HGF) receptor (Met) and presence of a truncated and activated intracellular HGF receptor fragment in locally aggressive/malignant human musculoskeletal tumors. Am J Pathol 2000;156:821–9.
28. Rutkowski P, Kaminska J, Kowalska M, Ruka W, Steffen J. Cytokine serum levels in soft tissue sarcoma patients: correlations with clinico-pathological features and prognosis. Int J Cancer 2002;100:463–71.
29. Garcia-Echeverria C, Pearson MA, Marti A, et al. *In vivo* antitumor activity of NVP-AEW541: a novel, potent, and selective inhibitor of the IGF-IR kinase. Cancer Cell 2004;5:231–9.
30. Nowell PC. Tumor progression: a brief historical perspective. Semin Cancer Biol 2002;12:261–6.
31. Scotting PJ, Walker DA, Perilongo G. Childhood solid tumours: a developmental disorder. Nat Rev Cancer 2005;5:481–8.
32. Wicha MS, Liu S, Dontu G. Cancer stem cells: an old idea-a paradigm shift. Cancer Res 2006;66:1883–90; discussion 1895–1886.
33. Perez-Losada J, Pintado B, Gutierrez-Adan A, et al. The chimeric FUS/TLS-CHOP fusion protein specifically induces liposarcomas in transgenic mice. Oncogene 2000;19:2413–22.
34. Jing S, Wen D, Yu Y, et al. GDNF-induced activation of the ret protein tyrosine kinase is mediated by GDNFR-alpha, a novel receptor for GDNF. Cell 1996;85:1113–24.
35. Khatib ZA, Matsushime H, Valentine M, Shapiro DN, Sherr CJ, Look AT. Coamplification of the CDK4 gene with MDM2 and GLI in human sarcomas. Cancer Res 1993;53:5535–41.
36. Heldin CH, Westermark B. Mechanism of action and *in vivo* role of platelet-derived growth factor. Physiol Rev 1999;79:1283–316.
37. Torchia EC, Jaishankar S, Baker SJ. Ewing tumor fusion proteins block the differentiation of pluripotent marrow stromal cells. Cancer Res 2003;63:3464–8.
38. Perez-Losada J, Sanchez-Martin M, Rodriguez-Garcia MA, et al. Liposarcoma initiated by FUS/TLS-CHOP: the FUS/TLS domain plays a critical role in the pathogenesis of liposarcoma. Oncogene 2000;19:6015–22.
39. Perez-Mancera PA, Perez-Losada J, Sanchez-Martin M, et al. Expression of the FUS domain restores liposarcoma development in CHOP transgenic mice. Oncogene 2002;21:1679–84.
40. Kuroda M, Ishida T, Takanashi M, Satoh M, Machinami R, Watanabe T. Oncogenic transformation and inhibition of adipocytic conversion of preadipocytes by TLS/FUS-CHOP type II chimeric protein. Am J Pathol 1997;151:735–44.
41. Braun BS, Frieden R, Lessnick SL, May WA, Denny CT. Identification of target genes for the Ewing's sarcoma EWS/FLI fusion protein by representational difference analysis. Mol Cell Biol 1995;15:4623–30.
42. Lessnick SL, Dacwag CS, Golub TR. The Ewing's sarcoma oncoprotein EWS/FLI induces a p53-dependent growth arrest in primary human fibroblasts. Cancer Cell 2002;1:393–401.
43. Deneen B, Denny CT. Loss of p16 pathways stabilizes EWS/FLI1 expression and complements EWS/FLI1 mediated transformation. Oncogene 2001;20:6731–41.
44. Naito Z. Role of the small leucine-rich proteoglycan (SLRP) family in pathological lesions and cancer cell growth. J Nippon Med Sch 2005;72:137–45.
45. Vuillermoz B, Khoruzhenko A, D'Onofrio MF, et al. The small leucine-rich proteoglycan lumican inhibits melanoma progression. Exp Cell Res 2004;296:294–306.

Expression of the FUS-CHOP Fusion Protein in Primary Mesenchymal Progenitor Cells Gives Rise to a Model of Myxoid Liposarcoma

Nicolò Riggi, Luisa Cironi, Paolo Provero, et al.

Cancer Res 2006;66:7016-7023.